

# Magnons in ultrathin ferromagnetic films with a large perpendicular magnetic anisotropy

H. J. Qin,<sup>1</sup> Kh. Zakeri,<sup>1,\*</sup> A. Ernst,<sup>1,2</sup> T.-H. Chuang,<sup>1</sup> Y.-J. Chen,<sup>1</sup> Y. Meng,<sup>1</sup> and J. Kirschner<sup>1,3</sup>

<sup>1</sup>Max-Planck-Institut für Mikrostrukturphysik, Weinberg 2, 06120 Halle, Germany

<sup>2</sup>Wilhelm Ostwald Institut für Physikalische und Theoretische Chemie, Universität Leipzig, Linnéstraße 2, 04103 Leipzig, Germany

<sup>3</sup>Institut für Physik, Martin-Luther-Universität Halle-Wittenberg, 06120 Halle, Germany

(Received 15 April 2013; published 15 July 2013)

We report on an experimental observation of high-energy magnon excitations in ultrathin ferromagnetic films with a perpendicular easy axis. We demonstrate that a transversally spin-polarized beam can be used to excite and probe the high-energy magnons within spin-polarized electron energy-loss spectroscopy experiments. The magnon dispersion relation and lifetime are probed over the entire surface Brillouin zone for a set of body-centered tetragonal FeCo films with a large perpendicular magnetic anisotropy. First-principles calculations reveal that in addition to the tetragonal distortion, which is the origin of the large perpendicular magnetic anisotropy, the interfacial electronic hybridization also has a considerable impact on the properties of magnons.

DOI: [10.1103/PhysRevB.88.020404](https://doi.org/10.1103/PhysRevB.88.020404)

PACS number(s): 75.30.Ds, 75.50.Bb, 75.70.Ak, 75.70.Rf

Ultrathin magnetic films with large perpendicular magnetic anisotropy (PMA) have attracted much attention due to their interesting fundamental properties and also their promising technological applications in ultrahigh-density magnetic recording,<sup>1,2</sup> magnetic tunneling junctions (MTJs),<sup>3</sup> and spin-transfer torque (STT) devices.<sup>4,5</sup> Because of their large PMA, these materials allow development of smaller magnetic elements with a high thermal stability. The STT devices fabricated by layers with PMA require a smaller switching current.

Many observed phenomena in the above-mentioned devices are attributed to the emission or absorption of interface magnons while performing transport experiments. For instance, the bias and temperature dependence of tunneling magnetoresistance in MTJs are attributed to the magnon emission and absorption by the tunneling hot electrons at the ferromagnet/insulator interface.<sup>6–8</sup> Although the magnon excitations are lying in the central point of explanation of all these phenomena, the full magnon spectrum of these materials is not known experimentally. Certainly, the knowledge on terahertz magnons would have a large impact on the understanding of many observed phenomena in the transport experiments as well as the ultrafast spin dynamics in these materials.

The experimental techniques enabling magnon investigation either do not have enough sensitivity, as in inelastic neutron scattering, or probe only a very narrow region of the momentum space close to the Brillouin zone center, as in Brillouin light scattering, and ferromagnetic resonance experiments. Recently, new experimental methods have been successfully applied to study magnetic excitations in low-dimensional magnets. They are based either on inelastic tunneling spectroscopy<sup>9</sup> or on spin-polarized electron energy loss spectroscopy (SPEELS).<sup>10,11</sup> Until now SPEELS has been used to study terahertz magnons in ultrathin films *with an in-plane easy axis*.<sup>10–20</sup> As the films with PMA possess an out-of-plane magnetic stray field, there has been a long-standing question concerning the possibility of probing magnons in these materials using SPEELS.

Here we report on an experimental observation of magnon excitations in a prototype PMA system, e.g., an ultrathin FeCo film (in the form of alloy as well as alternating Fe

and Co atomic layers). We will show how a transversally spin-polarized electron beam can be used to excite the magnons in an ultrathin film with a perpendicular easy axis. We demonstrate that the excitation probability (cross section) is rather strong such that one can easily excite and probe the magnons up to the surface Brillouin zone boundary and beyond. The dispersion relation and the lifetime of terahertz magnons in these materials are probed over the whole surface Brillouin zone. We show that the magnons' energies are rather low and their lifetimes are relatively short. Our first-principles calculations in the framework of density functional theory account for the explanation of the observed effects and provide us with information on the magnetic exchange parameters. We will also comment on the role of tetragonal distortion, which is the origin of large PMA in these materials, on the magnon dispersion relation.

The first main question to answer is: How might a transversally spin-polarized beam be used to excite the magnons? Let us assume a spin-polarized beam with an arbitrary polarization vector  $\mathbf{P} = |P|\mathbf{e}$ , where  $\mathbf{e} = \sin \vartheta \cos \varphi \hat{i} + \sin \vartheta \sin \varphi \hat{j} + \cos \vartheta \hat{k}$  is the unit vector in space indicating the direction of the spin-polarization vector [ $\vartheta$  and  $\varphi$  are the polar and azimuthal angles, respectively, and are defined with respect to the quantization axis; see Fig. 1(a)] and  $|P|$  is the norm of the polarization vector. The polarization vector of a given spin-polarized beam can be expressed in terms of Dirac spinors defining the spin-up and spin-down states.<sup>21</sup> This can be simply done by finding the eigenstates of

$$(\boldsymbol{\sigma} \cdot \mathbf{e})\chi = \lambda\chi, \quad (1)$$

where  $\boldsymbol{\sigma}$  represents the Pauli spin matrices and  $\boldsymbol{\sigma} \cdot \mathbf{e}$  is the projection of the spin operator in a polarization direction.  $\lambda$  and  $\chi$  represent the eigenvalue and the eigenstate of  $\boldsymbol{\sigma} \cdot \mathbf{e}$ , respectively. The solution of Eq. (1) is

$$\chi = \begin{pmatrix} \cos \frac{\vartheta}{2} \\ \sin \frac{\vartheta}{2} e^{i\varphi} \end{pmatrix} \quad \text{for } \lambda = +1, \quad (2)$$

$$\chi = \begin{pmatrix} \sin \frac{\vartheta}{2} \\ -\cos \frac{\vartheta}{2} e^{i\varphi} \end{pmatrix} \quad \text{for } \lambda = -1.$$

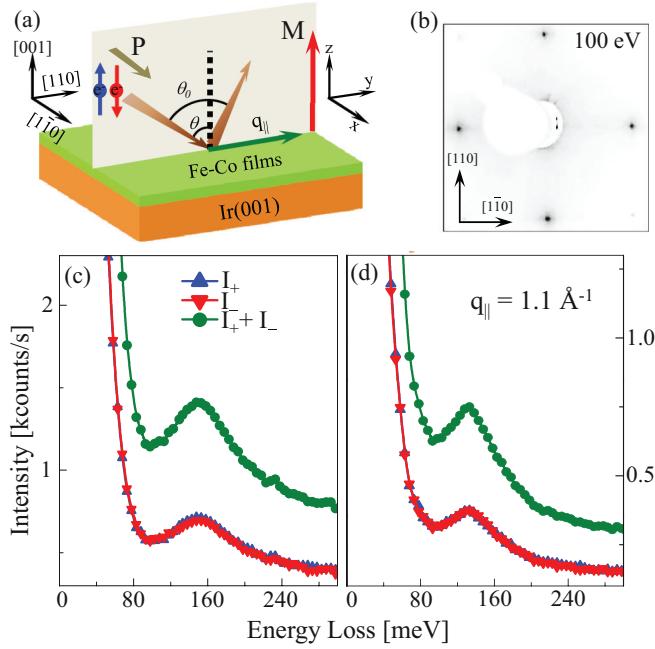


FIG. 1. (Color online) (a) A schematic representation of the scattering geometry. The beam polarization is either parallel or antiparallel to the  $[1\bar{1}0]$  direction (it is perpendicular to the quantization axis being the  $[001]$  direction). (b) A typical LEED pattern recorded on an ultrathin Fe<sub>0.5</sub>Co<sub>0.5</sub> alloy film with a thickness of 4 ML. SPEELS spectra recorded on the surfaces of a 4 ML Fe<sub>0.5</sub>Co<sub>0.5</sub> alloy film (c) and a 4 ML Fe/Co multilayer film (d) at a wave vector of  $q_{||} = 1.1 \text{ \AA}^{-1}$ .  $I_-$  ( $I_+$ ) indicates the intensity of the scattered electrons for the polarization vector of incident beam parallel (antiparallel) to the  $[1\bar{1}0]$  direction. The total spectrum is shown by  $I_+ + I_-$ . All the crystallographic directions depicted here are the ones of Ir(001).

For the case where  $\mathbf{P}$  is parallel or antiparallel to the magnetization (the quantization axis) one has  $\vartheta = 0, \varphi = 0$  [see Fig. 1(a)] and hence Eq. (1) yields the expected eigenstate of  $\sigma_z$ ,  $\begin{pmatrix} 1 \\ 0 \end{pmatrix}$  or  $\begin{pmatrix} 0 \\ 1 \end{pmatrix}$ .

For the case where  $\mathbf{P}$  is parallel or antiparallel to the  $x$  direction and the magnetization (the quantization axis) is along the  $z$  direction one has  $\vartheta = \pi/2, \varphi = 0$  and hence Eq. (1) yields the eigenstate  $\chi = \frac{1}{\sqrt{2}}\begin{pmatrix} 1/\sqrt{2} \\ 1 \end{pmatrix} = \frac{1}{\sqrt{2}}\begin{pmatrix} 1 \\ 0 \end{pmatrix} + \frac{1}{\sqrt{2}}\begin{pmatrix} 0 \\ 1 \end{pmatrix}$ , where,  $\begin{pmatrix} 1 \\ 0 \end{pmatrix}$  and  $\begin{pmatrix} 0 \\ 1 \end{pmatrix}$  are the Dirac spinors and can be regarded as majority and minority spin states of the sample, respectively. Note that in both examples the quantization axis is defined as the direction of the easy axis.

In our previous experiments, where  $\mathbf{P}$  was parallel or antiparallel to the quantization axis, the beam is composed of either majority or minority spins (assuming a polarization of 100%,  $|P| = 1$ ). In this case it is easy to think of an exchange process. An electron of minority character occupies a state above the Fermi level and another electron of majority character leaves the sample from a state below the Fermi level. Since the magnons carry a total angular momentum of  $1\hbar$ , they can only be excited by incident electrons of minority character via an exchange process. Hence one sees only the magnon excitation peak in minority spin spectra. Based on the discussion above, it is now rather straightforward to design

an experiment in which a transversally spin-polarized beam excites and probes magnons. In this case the beam can be regarded as a totally spin-unpolarized beam equally composed of both majority and minority spins. If the exchange process is valid here, only the incident electrons of minority character are allowed to excite magnons.<sup>20</sup> Since for both polarization directions (+ and -) the beam carries the same amount of majority and minority spins, one would expect exactly the same magnon peak intensity in  $I_+$  and  $I_-$  spectra. This would be another confirmation that the magnon excitation is caused by the exchange process, meaning that if one does the same experiment with positrons, one would not see the characteristic magnon energy losses.

To demonstrate that this idea works, we studied ultrathin magnetic FeCo-based films with large perpendicular magnetic anisotropy; systems which are of great fundamental as well as technological interest.<sup>3–5,22,23</sup> The experiments were carried out in an ultrahigh vacuum chamber with a base pressure of  $3 \times 10^{-11}$  mbar. The clean Ir(001) surface was obtained by cycles of low power flashes at 1200 K in oxygen atmosphere to remove the carbon contamination, followed by a single high power flash at 1800 K in ultrahigh vacuum, to remove the residual oxygen.<sup>24</sup> This preparation leads to a clean  $(1 \times 5)$ -Ir(001) surface as verified by low-energy electron diffraction (LEED) experiments. Two kinds of ultrathin films were grown following the procedure reported in Ref. 22: (i) an ultrathin Fe<sub>0.5</sub>Co<sub>0.5</sub> alloy film with a total thickness of four atomic layers (ML) prepared by codeposition of Fe and Co at room temperature and (ii) an ultrathin Fe/Co multilayer film composed of four alternating atomic layers of Co and Fe [starting with a Co layer; Fe/Co/Fe/Co/Ir(001)]. In both cases the films grow epitaxially with the epitaxial relationship  $[100]_{\text{film}} \parallel [110]_{\text{substrate}}$ . The sharp LEED patterns recorded on these surfaces indicate a high crystalline structure of the films [see, for example, Fig. 1(b)]. Both systems exhibit an out-of-plane easy axis due to the large PMA, originating from the tetragonal distortion of the epitaxial layers.<sup>22,23</sup> All measurements were carried out at room temperature. In the SPEELS measurements, the scattering plane was chosen to be parallel to the  $[110]$  direction of Ir(001) (the  $[010]$  direction of the films). The polarization vector of the beam  $\mathbf{P}$  is parallel (or antiparallel) to the  $[1\bar{1}0]$  direction of Ir(001). The degree of spin polarization of the incident electrons is  $|P| = 0.72 \pm 0.05$ . The energy of the incident electron beam was 8 eV. Different wave vectors were selected by changing the angle between incident and scattered beam, i.e., by rotating the sample about the symmetry axis  $[[1\bar{1}0]$  direction of Ir(001)]. In this configuration the effective beam polarization does not depend on the scattering geometry, since it is parallel to the symmetry axis. The wave vector of excited magnons parallel to the surface  $q_{||}$  is given by the scattering geometry:  $q_{||} = k_i \sin \theta - k_f \sin(\theta_0 - \theta)$ , where  $k_i$  ( $k_f$ ) is the magnitude of the wave vector of the incident (scattered) electrons and  $\theta$  ( $\theta_0$ ) is the angle between the incident beam and the sample normal (the scattered beam) [see Fig. 1(a)]. SPEELS spectra were recorded for the spin-polarization vector  $\mathbf{P}$  of the incident beam parallel and antiparallel to the  $[1\bar{1}0]$  direction of Ir(001), i.e., *perpendicular* to the quantization axis that is defined as the easy magnetization direction being normal to the sample plane (the  $[001]$  direction).

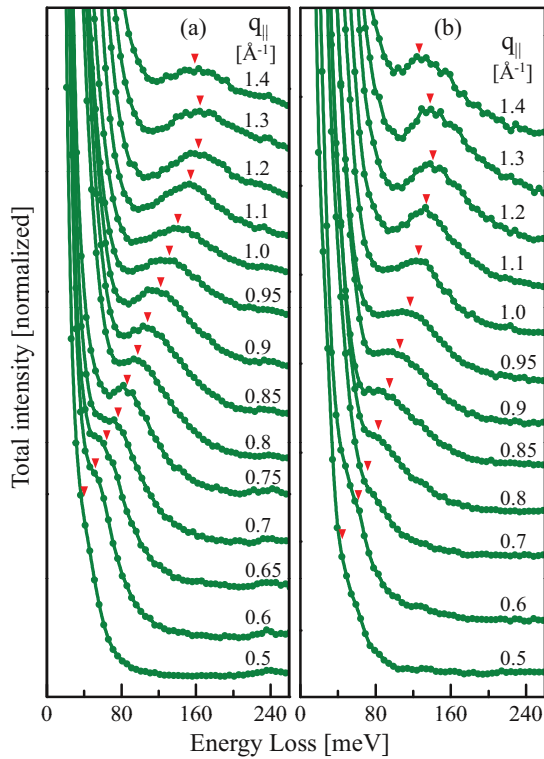


FIG. 2. (Color online) Series of normalized total spectra ( $I_+ + I_-$ ) recorded at different wave vectors along the  $\bar{\Gamma}$ - $\bar{X}$  direction on the surfaces of a 4 ML  $\text{Fe}_{0.5}\text{Co}_{0.5}$  alloy film (a) and a 4 ML Fe/Co multilayer film (b). The spectra are shifted upwards for a better comparison. The small triangles denote the magnon excitation energies.

Figures 1(c) and 1(d) show the  $I_+$  and  $I_-$  SPEELS spectra measured at a wave vector of  $1.1 \text{ \AA}^{-1}$  on the surfaces of a 4 ML  $\text{Fe}_{0.5}\text{Co}_{0.5}$  alloy film and a 4 ML Fe/Co multilayer film, respectively.  $I_+$  ( $I_-$ ) denotes the intensity of the scattered beam when  $\mathbf{P}$  is parallel (antiparallel) to the  $[1\bar{1}0]$  direction. On both surfaces, a pronounced peak appears in both  $I_+$  and  $I_-$  spectra with the same intensity and peak position. As expected, the peak intensity shows no dependence on the direction of  $\mathbf{P}$ , different than those recorded on the ultrathin films with in-plane magnetization.<sup>11,12</sup> This is due to the fact that unlike the previous experiments, where the beam polarization vector  $\mathbf{P}$  was parallel or antiparallel to magnetization direction (quantization axis), in the present case it is perpendicular to that.

A series of SPEELS total spectra recorded at different wave vectors along the  $\bar{\Gamma}$ - $\bar{X}$  direction are shown in Fig. 2. On both surfaces, the peak moves towards higher energies as the wave vector increases up to the zone boundary (at about  $1.2 \text{ \AA}^{-1}$ ). It moves towards lower energies when further increasing the wave vector. This is the indication of reaching the second Brillouin zone. As expected, the magnon energy starts decreasing beyond the first Brillouin zone because of the translational symmetry in the two-dimensional Brillouin zone. To completely describe the measured spectra, we fit them with a function which includes three Gaussians and one Voigt function. The Gaussians describe the quasielastic peak and the Rayleigh surface phonons and the Voigt func-

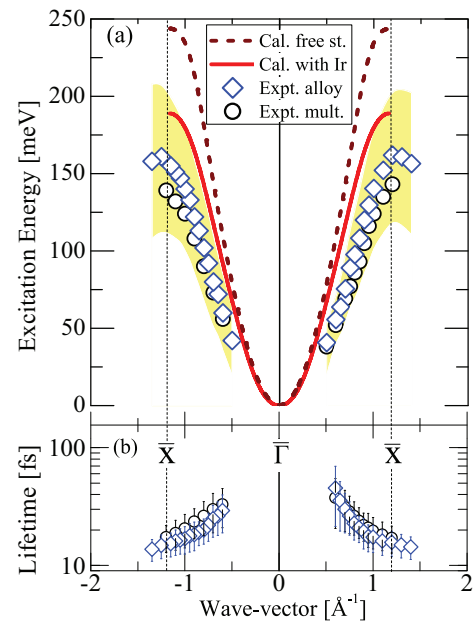


FIG. 3. (Color online) (a) The magnon dispersion relation probed along the  $\bar{\Gamma}$ - $\bar{X}$  direction on a 4 ML  $\text{Fe}_{0.5}\text{Co}_{0.5}$  alloy film ( $\diamond$ ) and a 4 ML Fe/Co multilayer film ( $\circ$ ). The intrinsic linewidth of the spectra is depicted as the background color. The solid line represents the theoretical calculation for a 4 ML body-centered tetragonal FeCo film on Ir(001) composed of alternating layers of Co and Fe. The layer next to Ir(001) is a Co layer (as in the experiment). The dashed line represents the results of the calculations for a freestanding film. (b) The magnon lifetime as a function of the wave vector.

tion describes the magnon peak.<sup>17,25</sup> In the Voigt function, the linewidth of the Gaussian contribution is chosen to be the same as the experimental resolution (the linewidth of the quasielastic peak). The peak position denotes the magnon energy and the intrinsic linewidth provides information on the magnon lifetime.<sup>26</sup> Due to the large contribution of the quasielastic peak in the spectra at the wave vectors smaller than  $0.5 \text{ \AA}^{-1}$  it is rather difficult to extract the magnon excitation energy. The only nonmagnetic excitations which are in the same energy range as magnons are the vibrational excitations of adsorbed atoms or molecules. For example, the narrow and very weak peak around 240 meV in Fig. 1(c) corresponds to the vibrational excitations of CO molecules. As the experiments are performed under ultrahigh vacuum conditions, the vibrational excitations are very weak so that their influence on the magnon peak can be neglected.

The magnon dispersion relation measured on both  $\text{Fe}_{0.5}\text{Co}_{0.5}$  alloy and Fe/Co multilayer films is presented in Fig. 3(a). At low wave vectors both systems possess almost identical magnon energies. Small differences in magnon energies appear at high wave vectors. For the  $\text{Fe}_{0.5}\text{Co}_{0.5}$  alloy film, the energy reaches a value of 160 meV at the  $\bar{X}$  point; for the Fe/Co multilayer film, the energy is about 140 meV. In both cases the magnon energies are much smaller than the one in bulk Fe and Co. They are even smaller than the one of 2 ML Fe(110)/W(110)<sup>12</sup> and 8 ML Co(001)/Cu(001).<sup>11</sup> Recent calculations of tetragonally distorted bulk FeCo compounds within the many-body perturbation theory predict a magnon softening.<sup>27</sup> Due to technical difficulties in those calculations

the effects of the substrate, which seem to be important, could not be taken into consideration.

We perform first-principles calculations within the generalized gradient approximation of the density functional theory. The structural parameters are taken from the available experimental data.<sup>28,29</sup> The electronic and magnetic properties are calculated using a self-consistent Green function method, specially designed for layered structures.<sup>30</sup> The interatomic exchange parameters were determined employing the magnetic force theorem, implemented within the Green function method.<sup>31</sup> The results of calculations are presented in Fig. 3(a) showing a rather good agreement with the experimental data. The small differences between the calculated dispersion relation and the experimental results might be due to different reasons. The intermixing of Fe and Co resulting in a chemically disordered alloy might be the first reason. The second reason might be a deviation from the perfect multilayer structure due to uncertainties in the thickness of Fe and Co layers and also a nonperfect (layer-by-layer) growth mode of Fe and Co layers on Ir(001). We also noticed that the calculations based on local spin density approximation results in magnon energies which are slightly smaller than the ones calculated within the generalized gradient approximation (they are very similar to the experimental results).

To see the impact of the Ir(001) substrate on the magnon dispersion relation we performed calculations for a freestanding film taking the interatomic distances the same as the film with substrate. The results, shown in Fig. 3(a) as a dashed line, indicate that the role of the substrate in determining the magnon energies is very important. The presence of the Ir(001) substrate reduces the magnon energies by 55 meV at the  $\bar{X}$  point. This fact is the consequence of the weakening of the interatomic exchange interaction and beautifully manifests the importance of electronic hybridization of the ultrathin film and the substrate. Detailed analysis of exchange coupling constants reveals that mainly the nearest-neighbor and next-nearest-neighbor coupling constants of Co atoms sitting next to Ir substrate are reduced by a factor of 2 in the presence of the substrate. This reduction is due to the reconstruction of the electronic structures of the film in contact with the substrate.

The background color in Fig. 3(a) denotes the intrinsic linewidth of the magnon peaks as observed in the experiments.

Since they are very similar in both systems we only show the results of the alloy film. The intrinsic linewidth increases from 40 to 100 meV when the wave vector increases from 0.5 to 1.2  $\text{\AA}^{-1}$ , similar to that of an 8 ML Co/Cu(100) and a 2 ML Fe/W(110).<sup>25</sup> The magnon lifetime is obtained using the procedure explained in Refs. 25 and 17 and is presented in Fig. 3(b). The damping of magnons in itinerant ferromagnets is mainly governed by the decay of collective excitations into single-particle Stoner excitations.<sup>25,32,33</sup> This damping mechanism which is usually referred to as Landau damping depends strongly on the available Stoner states near the Fermi level. Due to strong damping, terahertz magnons possess a very short lifetime being in the order of a few tens of femtoseconds.<sup>17,25</sup> The lifetime of FeCo with large PMA is very similar to that of the Fe and Co films meaning that the tetragonal distortion does not significantly influence the magnons lifetime. A large damping of magnons in the tetragonally distorted bulk FeCo compounds is also predicted theoretically.<sup>27</sup>

In conclusion, we demonstrate that the high-energy magnons in ultrathin ferromagnetic films with an out-of-plane easy axis can be probed by a transversally spin-polarized beam. The excitation cross section is rather large so that a pronounced peak in the spectra can be observed. Since ultrathin films with PMA are of great fundamental and technological interest, our experiments would open a way towards investigation of magnon excitations in this class of materials by SPEELS and also by inelastic tunneling spectroscopy.<sup>9</sup> The magnon dispersion relation and lifetime of tetragonally distorted ultrathin FeCo films with large PMA are probed. Our first-principles calculations reveal that in addition to the tetragonal distortion, the interfacial electronic hybridizations play an important role in determining the magnon energies in these compounds. We anticipate that our results would have an impact on the understanding of phenomena related to spin dynamics in these materials.

Funding from the Deutsche Forschungsgemeinschaft is acknowledged by A.E. (DFG priority program SPP 1538 “Spin Caloric Transport”). The calculations were performed at the Rechenzentrum Garching of the Max Planck Society (Germany).

\*zakeri@mpi-halle.de

<sup>1</sup>D. Weller, A. Moser, L. Folks, M. E. Best, W. Lee, M. F. Toney, M. Schwickert, J.-U. Thiele, and M. F. Doerner, *IEEE Trans. Magn.* **36**, 10 (2000).

<sup>2</sup>A. Moser, K. Takano, D. T. Margulies, M. Albrecht, Y. Sonobe, Y. Ikeda, S. Sun, and E. E. Fullerton, *J. Phys. D: Appl. Phys.* **35**, R157 (2002).

<sup>3</sup>S. Ikeda, K. Miura, H. Yamamoto, K. Mizunuma, H. D. Gan, M. Endo, S. Kanai, J. Hayakawa, F. Matsukura, and H. Ohno, *Nat. Mater.* **9**, 721 (2010).

<sup>4</sup>L. Liu, C.-F. Pai, Y. Li, H. W. Tseng, D. C. Ralph, and R. A. Buhrman, *Science* **336**, 555 (2012).

<sup>5</sup>L. Liu, O. J. Lee, T. J. Gudmundsen, D. C. Ralph, and R. A. Buhrman, *Phys. Rev. Lett.* **109**, 096602 (2012).

<sup>6</sup>S. Zhang, P. M. Levy, A. C. Marley, and S. S. P. Parkin, *Phys. Rev. Lett.* **79**, 3744 (1997).

<sup>7</sup>X.-F. Han, A. C. C. Yu, M. Oogane, J. Murai, T. Daibou, and T. Miyazaki, *Phys. Rev. B* **63**, 224404 (2001).

<sup>8</sup>P. M. Levy and A. Fert, *Phys. Rev. Lett.* **97**, 097205 (2006).

<sup>9</sup>T. Balashov, A. F. Takacs, W. Wulfhekel, and J. Kirschner, *Phys. Rev. Lett.* **97**, 187201 (2006).

<sup>10</sup>H. Ibach, D. Bruchmann, R. Vollmer, M. Etzkorn, P. S. A. Kumar, and J. Kirschner, *Rev. Sci. Instrum.* **74**, 4089 (2003).

<sup>11</sup>R. Vollmer, M. Etzkorn, P. S. Anil Kumar, H. Ibach, and J. Kirschner, *Phys. Rev. Lett.* **91**, 147201 (2003).

<sup>12</sup>W. X. Tang, Y. Zhang, I. Tudosa, J. Prokop, M. Etzkorn, and J. Kirschner, *Phys. Rev. Lett.* **99**, 087202 (2007).



- <sup>13</sup>J. Prokop, W. X. Tang, Y. Zhang, I. Tudosa, T. R. F. Peixoto, K. Zakeri, and J. Kirschner, *Phys. Rev. Lett.* **102**, 177206 (2009).
- <sup>14</sup>K. Zakeri, Y. Zhang, J. Prokop, T.-H. Chuang, N. Sakr, W. X. Tang, and J. Kirschner, *Phys. Rev. Lett.* **104**, 137203 (2010).
- <sup>15</sup>Y. Zhang, P. A. Ignatiev, J. Prokop, I. Tudosa, K. Zakeri, V. S. Stepanyuk, J. Kirschner, T. R. F. Peixoto, and W. X. Tang, *Phys. Rev. Lett.* **106**, 127201 (2011).
- <sup>16</sup>H. Ibach, J. Rajeswari, and C. M. Schneider, *Rev. Sci. Instrum.* **82**, 123904 (2011).
- <sup>17</sup>K. Zakeri, Y. Zhang, T.-H. Chuang, and J. Kirschner, *Phys. Rev. Lett.* **108**, 197205 (2012).
- <sup>18</sup>T.-H. Chuang, K. Zakeri, A. Ernst, L. M. Sandratskii, P. Buczek, Y. Zhang, H. J. Qin, W. Adeagbo, W. Hergert, and J. Kirschner, *Phys. Rev. Lett.* **109**, 207201 (2012).
- <sup>19</sup>J. Rajeswari, H. Ibach, C. M. Schneider, A. T. Costa, D. L. R. Santos, and D. L. Mills, *Phys. Rev. B* **86**, 165436 (2012).
- <sup>20</sup>K. Zakeri and J. Kirschner, in *Probing Magnons by Spin-Polarized Electrons*, Topics in Applied Physics Magnonics from Fundamentals to Applications, Vol. 125 (Springer, Berlin, Heidelberg, 2013), Chap. 7, pp. 84–99.
- <sup>21</sup>J. Kesseler, *Polarized Electrons* (Springer, Berlin, 1985).
- <sup>22</sup>F. Yildiz, M. Przybylski, X.-D. Ma, and J. Kirschner, *Phys. Rev. B* **80**, 064415 (2009).
- <sup>23</sup>T. Burkert, L. Nordström, O. Eriksson, and O. Heinonen, *Phys. Rev. Lett.* **93**, 027203 (2004).
- <sup>24</sup>K. Zakeri, T. Peixoto, Y. Zhang, J. Prokop, and J. Kirschner, *Surf. Sci.* **604**, L1 (2010).
- <sup>25</sup>Y. Zhang, T.-H. Chuang, K. Zakeri, and J. Kirschner, *Phys. Rev. Lett.* **109**, 087203 (2012).
- <sup>26</sup>See Supplemental Material at <http://link.aps.org/supplemental/10.1103/PhysRevB.88.020404> for detailed information on the fitting procedure of the experimental data.
- <sup>27</sup>E. Sasioglu, C. Friedrich, and S. Blugel, *Phys. Rev. B* **87**, 020410 (2013).
- <sup>28</sup>V. Martin, W. Meyer, C. Giovanardi, L. Hammer, K. Heinz, Z. Tian, D. Sander, and J. Kirschner, *Phys. Rev. B* **76**, 205418 (2007).
- <sup>29</sup>K. Heinz and L. Hammer, *Prog. Surf. Sci.* **84**, 2 (2009).
- <sup>30</sup>M. Lüders, A. Ernst, W. M. Temmerman, Z. Szotek, and P. J. Durham, *J. Phys.: Condens. Matter* **13**, 8587 (2001).
- <sup>31</sup>A. I. Liechtenstein, M. I. Katsnelson, V. P. Antropov, and V. A. Gubanov, *J. Magn. Magn. Mater.* **67**, 65 (1987).
- <sup>32</sup>A. T. Costa, R. B. Muniz, and D. L. Mills, *Phys. Rev. B* **74**, 214403 (2006).
- <sup>33</sup>P. Buczek, A. Ernst, and L. M. Sandratskii, *Phys. Rev. Lett.* **106**, 157204 (2011).